

Vorticity alignment results for the three-dimensional Euler and Navier–Stokes equations

B Galanti^{†§}, J D Gibbon^{†‡||} and M Heritage[‡]

[†] Department of Chemical Physics, Weizmann Institute of Science, 76100 Rehovot, Israel

[‡] Department of Mathematics, Imperial College of Science, Technology and Medicine, London SW7 2BZ, UK

Received 14 July 1997

Recommended by I Proccacia

Abstract. We address the problem in Navier–Stokes isotropic turbulence of why the vorticity accumulates on thin sets such as quasi-one-dimensional tubes and quasi-two-dimensional sheets. Taking our motivation from the work of Ashurst, Kerstein, Kerr and Gibbon, who observed that the vorticity vector ω aligns with the intermediate eigenvector of the strain-matrix S , we study this problem in the context of both the three-dimensional Euler and Navier–Stokes equations using the variables $\alpha = \hat{\xi} \cdot S\hat{\xi}$ and $\chi = \hat{\xi} \times S\hat{\xi}$ where $\hat{\xi} = \omega/\omega$. This introduces the dynamic angle $\phi(x, t) = \arctan(\frac{\chi}{\alpha})$, which lies between ω and $S\omega$. For the Euler equations a closed set of differential equations for α and χ is derived in terms of the Hessian matrix of the pressure $P = \{p_{,ij}\}$. For the Navier–Stokes equations, the Burgers vortex and shear-layer solutions turn out to be the Lagrangian fixed-point solutions of the equivalent (α, χ) equations with a corresponding angle $\phi = 0$. Under certain assumptions for more general flows it is shown that there is an attracting fixed point of the (α, χ) equations which corresponds to positive vortex stretching and for which the cosine of the corresponding angle is close to unity. This indicates that near alignment is an attracting state of the system and is consistent with the formation of Burgers-like structures.

AMS classification scheme numbers: 76F05, 76C05

PACS numbers: 4727J, 4732C, 4715K

1. Introduction

As early as 1938 Taylor [1] showed that, in isotropic Navier–Stokes turbulence, vortex stretching has a major effect on vorticity production and dissipation. One of the many interesting features of high Reynolds number turbulent flows, illustrated beautifully by modern flow-visualization methods, is the fact that vorticity is not evenly distributed throughout a flow but has a tendency to accumulate on ‘thin sets’. The morphology of these sets is characterized by the predominance of quasi one-dimensional tubes or filaments and quasi two-dimensional sheets although, being fractal in nature [2–4], many individual vortical structures may be neither precisely one nor the other. This morphology makes it clear that the *direction* of vorticity, as well as its production, plays a significant role in the self-organization processes through which apparently intense regions of vorticity appear to

§ E-mail address: galanti@dvir.weizmann.ac.il

|| E-mail address: j.gibbon@ic.ac.uk

metamorphose into approximate thin coherent structures. The challenge facing the theorist working with the three-dimensional Navier–Stokes equations is to explain these geometric accumulation processes and their consequences even though a detailed description of their precise topology is beyond our reach at present. The subtle fine spatial structure of these sets indicates that an alternative approach is needed to the conventional one of Navier–Stokes analysis where L^2 -spatial averages are taken over the whole domain when estimating the effect of the vortex-stretching term.

In 1951, Townsend [5, 6] indicated that something like the thin sets described above might be relevant in turbulent flows and in the last two decades their occurrence has been a regular theme of the literature [7–28]. They would also seem to be the visual manifestation of the vorticity-alignment phenomenon first reported by Ashurst *et al* [14] who observed that, in driven simulated isotropic Navier–Stokes turbulence with a Taylor microscale Reynolds number of 83, the vorticity vector ω has a tendency to align with the intermediate eigenvector of the rate-of-strain matrix

$$S_{ij} = \frac{1}{2}(u_{i,j} + u_{j,i}). \quad (1)$$

This observation was based on a study of the probability density function (PDF) of the cosine of the angle between their directions. This important alignment process has also been confirmed in other numerical simulations [15, 16, 18, 20, 26, 28] as well as in turbulent-grid flow experiments conducted by Tsinober *et al* [29–32] and it has been suggested that it is a kinematic process [33, 34]. In fact preferential vorticity alignment appears to be a universal feature of smaller-scale structures in such flows even though larger-scale features may vary from flow to flow. A common feature seems to be that vorticity is concentrated in tubes of width intermediate between the Taylor and Kolmogorov microscales [14, 16, 18, 20, 28] with viscous dissipation occurring in annular regions around the tubes which themselves form from the roll-up of vortex sheets [26].

In isolation from each other and in an ideal sense, vortex tubes and sheets can be thought of as Burgers vortices and Burgers (stretched) shear layers respectively for which there are known exact solutions of the Navier–Stokes equations in certain special cases [25, 13, 24, 35]. Of course the Burgers solutions are idealized because their strain fields are not linked back to the local vorticity field as would be the case in a real flow. Nevertheless they have the great merit of providing us with exact solutions which allow an interpretation of the processes involved. A Burgers vortex tube ideally has one positive and two negative eigenvalues of the strain matrix (axial strain) while a Burgers shear-layer solution has two positive and one negative eigenvalues (biaxial strain). Ashurst *et al* [14] reported that their eigenvalues occurred in the ratio 3 : 1 : –4 but, as Moffatt *et al* [25] have pointed out, vortex tubes can still survive in regions of biaxial strain provided they are strong enough. As best illustrated by the graphics of Vincent and Meneguzzi [26], vortex sheets deform neighbouring sheets, curling up like potato crisps (chips), most strongly when rolling up into tubes. It is significant that they found that the tendency towards alignment between ω and the intermediate eigenvector of S occurred before the roll-up of sheets into tubes. Burgers vortices have been produced in the laboratory by Andreotti *et al* [36] from two experimental set-ups which allow them to study the phenomenon of vortex stretching in detail. While the Burgers solutions are extremely valuable to the theorist, it is necessary to formulate a theory which demonstrates why a flow should evolve to such states in the first place.

For the three-dimensional Euler equations the situation is somewhat different and complicated by the suspicion of a finite-time singularity in the vorticity field (see [37, 38]). Constantin *et al* [39, 40], however, have recently shown that singularities in solutions of

the three-dimensional incompressible Euler equations can be ruled out if the velocity is finite and the direction of vorticity is smooth but they cannot be ruled out if the direction of vorticity is not smooth. For instance, blow-up cannot be ruled out if two intense vortex tubes collide at a nontrivial angle. In fact, Kerr’s computations predicting such a singularity used antiparallel vortex tubes as initial data [37, 38] (see also [41, 42]). The result of Constantin *et al* [39] is related to that of Beale *et al* [43] which has provided the main criterion for understanding the growth of vorticity in Euler flows for more than a decade.

We begin by setting up the notation and then proceed to give some preliminary definitions. Let us consider the incompressible three-dimensional Euler equations in vorticity form

$$\frac{D\omega}{Dt} = \sigma \quad (2)$$

and the Navier–Stokes equations

$$\frac{D\omega}{Dt} = \sigma + \nu \Delta \omega \quad (3)$$

with a divergence-free velocity field $\operatorname{div} \mathbf{u} = 0$. The material derivative is defined in the usual manner as

$$\frac{D}{Dt} = \frac{\partial}{\partial t} + \mathbf{u} \cdot \nabla. \quad (4)$$

The vortex stretching vector σ appearing in (2) and (3) is given by

$$\sigma_i = \omega_j u_{i,j} = S_{ij} \omega_j. \quad (5)$$

σ is written as $\sigma = S\omega$ on the right-hand side of (5) because ω sees only the symmetric part of $u_{i,j}$. The approach taken in this paper is to consider the dynamics of the local angle $\phi(\mathbf{x}, t)$ which lies between the vorticity vector ω and $S\omega$ at the point \mathbf{x} . Not having independent evolution equations for the eigenvectors of S restricts our ability to interpret the geometry of the problem. The significance of ϕ in this context is that when it takes the value(s) $\phi = 0(\pi)$ this means that ω has aligned (anti-aligned) with an eigenvector of S , although which one we cannot say. The so-called ‘stretching rate’ α is an interesting quantity to consider ($\hat{\xi} = \omega/|\omega|$)

$$\alpha(\mathbf{x}, t) = \frac{\omega \cdot \sigma}{\omega \cdot \omega} = \frac{\omega \cdot S\omega}{\omega \cdot \omega} = \hat{\xi} \cdot S\hat{\xi} \quad (6)$$

which has been related to the vorticity through an elegant Biot–Savart integral [39, 40]. For the three-dimensional Euler equations, the scalar vorticity $\omega = |\omega|$ simply obeys

$$\frac{D\omega}{Dt} = \alpha\omega. \quad (7)$$

The scalar α is obviously an estimate for an eigenvalue of the strain matrix S and lies within its spectrum. By defining the vector

$$\chi(\mathbf{x}, t) = \frac{\omega \times S\omega}{\omega \cdot \omega} = \hat{\xi} \times S\hat{\xi} \quad (8)$$

the angle $\phi(\mathbf{x}, t)$ between ω and $S\omega$ can naturally be introduced as ($\chi \cdot \chi = \chi^2$)

$$\tan \phi(\mathbf{x}, t) = \frac{|\omega \times S\omega|}{\omega \cdot S\omega} = \frac{\chi}{\alpha} \quad (9)$$

and its dynamics related to those of α and χ . Gibbon and Heritage [44] have recently discussed this angle but only in the context of the volume average over the whole flow. The stretching rate α takes account only of the symmetric part S of the deformation matrix

$u_{i,j}$ but the antisymmetric part clearly contributes to χ . For a fluid element at a point \mathbf{x} certain specific values of the angle ϕ can be interpreted as the following.

- (1) When $\phi = 0$ the vectors $\boldsymbol{\omega}$ and $S\boldsymbol{\omega}$ are parallel and only stretching occurs.
- (2) When $\phi = \pi/2$ the vectors $\boldsymbol{\omega}$ and $S\boldsymbol{\omega}$ are orthogonal and, since $S\boldsymbol{\omega} = D\boldsymbol{\omega}/Dt$, this means that in this case $\boldsymbol{\omega}$ rotates but does not stretch. This effect will nevertheless distend and misalign vortex lines.
- (3) The case $\phi = \pi$ represents anti-alignment. In this case $\alpha < 0$, so vorticity collapses rapidly to small values.
- (4) When $0 < \phi < \pi/2$ both stretching and rotation occur simultaneously at each point on a vortex line.

In order to find the most sensitive relationship between α and χ we take advantage in section 2 of a result of Ohkitani [46, 47] for the incompressible three-dimensional Euler equations:

$$\frac{D\boldsymbol{\sigma}}{Dt} = -P\boldsymbol{\omega} \quad (10)$$

where $P = \{p_{,ij}\}$ is the Hessian matrix of the pressure. This result (see first note added in proof) comes about from a more general well known property of the Euler equations, namely that if \mathbf{u} and $\boldsymbol{\omega}$ are velocity and vorticity solutions of the Euler equations then for any arbitrary vector \mathbf{A}

$$\frac{D}{Dt} \left(\omega_j \frac{\partial A_i}{\partial x_j} \right) = \sigma_j \frac{\partial A_i}{\partial x_j} - \sigma_k \frac{\partial A_i}{\partial x_k} + \omega_j \frac{\partial}{\partial x_j} \frac{DA_i}{Dt} \quad (11)$$

from which we conclude that

$$\frac{D}{Dt} (\boldsymbol{\omega} \cdot \nabla \mathbf{A}) = \boldsymbol{\omega} \cdot \nabla \left(\frac{D\mathbf{A}}{Dt} \right). \quad (12)$$

Choosing $\mathbf{A} = \mathbf{u}$ with a direct use of the velocity form of the Euler equations on the right-hand side of equation (12) immediately gives equation (10). While the pressure Hessian in (10) is a fully nonlinear term ($\text{tr}P$ is related to $u_{i,j}$ by $\Delta p = -u_{i,j}u_{j,i}$), nevertheless the cancellation of two terms inherent in the derivation of equation (10), each of which are $\sim \boldsymbol{\omega}|\nabla \mathbf{u}|^2$, directly removes all the terms not explicitly dependent on P . The approach of this paper therefore runs counter to the conventional one where the pressure is removed by projection but the advantage gained by the fortuitous cancellation of nonlinear terms comes at the price of having to deal with the P -matrix. Previous studies on depletion of nonlinearity have been made by Constantin and Fefferman [45] for the three-dimensional Navier–Stokes equations and Constantin *et al* [39] for the three-dimensional Euler equations who have considered the angle between the vorticity vectors $\boldsymbol{\omega}(\mathbf{x})$ and $\boldsymbol{\omega}(\mathbf{y})$ at two points \mathbf{x} and \mathbf{y} in the flow.

The main results of the paper can be summarized as follows. It is shown in section 2 that at points in the flow for which $\boldsymbol{\omega} \neq 0$, the material derivatives of α and χ for the Euler equations obey

$$\frac{D\alpha}{Dt} = \chi^2 - \alpha^2 - \alpha_p \quad (13)$$

$$\frac{D\chi}{Dt} = -2\alpha\chi - \chi_p \quad (14)$$

where α_p and χ_p are related to the Hessian matrix P which is a non-local quantity in the flow [47–49]. For the Navier–Stokes equations (see section 3) the addition of viscosity

produces differential equations of the type

$$\frac{D\alpha}{Dt} = \chi^2 - \alpha^2 + \nu\Delta\alpha + 2\nu\alpha|\nabla\hat{\xi}|^2 + \lambda \tag{15}$$

$$\frac{D\chi}{Dt} = -2\alpha\chi + \nu\Delta\chi + 2\nu\chi|\nabla\hat{\xi}|^2 + \mu \tag{16}$$

where the terms in $|\nabla\hat{\xi}|^2$ express the misalignment of vortex lines in the differential geometric sense [50, 51]. The terms λ and μ contain information about the flow and are not generally constant. In section 4, however, the exact solutions of the Navier–Stokes equations that represent Burgers vortex tubes and shear layers are discussed and it is discovered there that these correspond to ‘Lagrangian fixed-point’ solutions of (15) and (16) in the sense that $D\alpha/Dt = 0$ and $D\chi/Dt = 0$, λ and α are positive real constants and $\mu = 0$ and $\chi = 0$. Hence for both these thin structures λ and μ simplify greatly and the corresponding angle ϕ is exactly zero. Using this as motivation, it is assumed in section 5 that if the flow is regular then all the variables must come to some equilibrium in a connected region of high vorticity. From this we want to see if the equilibrium values of α and χ correspond to a *small* angular orientation ϕ_0 . In order to do this it is assumed that λ and μ are constant and then it is shown that equations (15) and (16) have two fixed-point solutions (α_0, χ_0) in the Lagrangian sense, one of which is repelling ($\alpha_0 < 0$) while the other ($\alpha_0 > 0$) is attracting. The stability of the positive root for α shows that the system favours vortex stretching, in agreement with Taylor’s conclusions [1]. For $\lambda > 0$, the stable solution has a corresponding small attracting angle ϕ_0 which is insensitive to the relative ratio of λ and $|\mu|$, making the natural orientation of the vectors close to true alignment. These results are consistent with near Burgers-like structures forming in the flow. It remains to be proved, however, that the Burgers solutions are either unique or belong to a more general unique class of solutions that correspond to thin sets which are true Lagrangian fixed points with small values of ϕ . As we point out in section 2 neither Hill’s spherical vortex (an exact solution of the Euler equations) nor ABC flow belong to the class we are considering as neither are Lagrangian fixed points of their respective (α, χ) equations.

2. Stretching equations for the three-dimensional Euler equations

The scalar α and the vector χ were defined in equations (6) and (8) by forming the dot and cross products respectively of ω with $S\omega$. We repeat their definitions:

$$\alpha = \frac{\omega \cdot S\omega}{\omega \cdot \omega} = \hat{\xi} \cdot S\hat{\xi} \quad \chi = \frac{\omega \times S\omega}{\omega \cdot \omega} = \hat{\xi} \times S\hat{\xi} \tag{17}$$

but exclude points where $\omega = 0$. The unit vector $\chi(x, t)$, defined by

$$\hat{\chi} = \frac{\chi}{\chi} \tag{18}$$

is orthogonal to the unit vector $\hat{\xi}$; for example, if $\hat{\xi}$ points along a vortex tube then $\hat{\chi}$ lies in the plane orthogonal to the tube. Let us also define the scalar quantity α_p and the vector χ_p

$$\alpha_p(x, t) = \frac{\omega \cdot P\omega}{\omega \cdot \omega} \quad \chi_p(x, t) = \frac{\omega \times P\omega}{\omega \cdot \omega}. \tag{19}$$

α_p is an estimate for an eigenvalue of the Hessian of the pressure $P = \{p_{,ij}\}$ in the same way that α is for the strain-matrix S . When ω aligns with an eigenvector of P then α_p becomes an exact eigenvalue of P whereas χ_p becomes zero in this case.

In section 1 the definitions (6) and (8) were used to define the angle ϕ between ω and $\sigma = S\omega$, namely $\tan \phi = \chi/\alpha$, as a way of characterizing the alignment or misalignment between them. In terms of the vector $\hat{\chi}$ this angle obeys ($\sigma = S\omega$)

$$\hat{\chi} \tan \phi = \frac{\omega \times \sigma}{\omega \cdot \sigma} = \frac{\omega \times S\omega}{\omega \cdot S\omega} \quad (20)$$

with ϕ varying in the range $0 \leq \phi \leq 2\pi$. One consequence of equation (20) is that

$$\cos^2 \phi = \frac{(\sigma \cdot \omega)^2}{|\sigma|^2 |\omega|^2} = \frac{\omega^2 \alpha^2}{\sigma^2}. \quad (21)$$

To obtain relations between these quantities we first note that

$$\frac{D(\omega \cdot \sigma)}{Dt} = \sigma^2 - \omega \cdot P\omega = \omega^2 (\alpha^2 \sec^2 \phi - \alpha_p). \quad (22)$$

whereas in the cross product, the terms in σ vanish leaving only

$$\frac{D(\omega \times \sigma)}{Dt} = -\omega \times P\omega. \quad (23)$$

Equation (23) shows that in addition to the cancellation of nonlinear terms in Ohkitani's relation, more nonlinearity has been lost through the cross product. The material derivatives of α and χ can now easily be obtained through equations (6), (21)–(23),

$$\frac{D\alpha}{Dt} = \chi^2 - \alpha^2 - \alpha_p \quad (24)$$

$$\frac{D\chi}{Dt} = -2\alpha\chi - \chi_p. \quad (25)$$

Subject to solutions existing, the prominent feature of (24) and (25) is that they are independent explicitly of ω and ϕ while being driven by $\alpha_p(x, t)$ and $\chi_p(x, t)$. Hence they are a set of nonautonomous ODEs, in the Lagrangian picture of fluid mechanics, operating in a four-dimensional phase space (α, χ_i) for $i = 1, 2, 3$. The three equations in the χ_i can be reduced to one in the scalar $\chi = \sqrt{\chi \cdot \chi}$ to give the pair of equations

$$\frac{D\alpha}{Dt} = \chi^2 - \alpha^2 - \alpha_p \quad (26)$$

$$\frac{D\chi}{Dt} = -2\alpha\chi - \tilde{\chi}_p \quad (27)$$

where

$$\tilde{\chi}_p = \hat{\chi} \cdot \chi_p. \quad (28)$$

On the α -axis where $\phi = 0$ or π , equation (23) show that $\omega \times P\omega = 0$. Hence $\chi_p = 0$ and so $D\chi/Dt = 0$ on this axis. Consequently equation (27) operates only in the the upper half-plane. The lower half-plane is simply a reflection of the upper in the α -axis. While α is the stretching rate for the scalar vorticity ω , equation (27) shows that 2α is the contraction rate for χ with an additional pressure term. The two scalars ω and χ are also related by

$$\frac{D^2\omega}{Dt^2} = (\chi^2 - \alpha_p)\omega. \quad (29)$$

The pair of equations for (α, χ) given above can be merged into one by defining the complex stretching rate

$$\zeta = \alpha + i\chi \quad (30)$$

and (26) and (27) reduce to

$$\frac{D\zeta}{Dt} + \zeta^2 + \zeta_p = 0. \tag{31}$$

ζ_p is simply the complex combination $\zeta_p = \alpha_p + i\tilde{\chi}_p$. Because the ζ -plane is only the upper half of the complex plane, ϕ is valid only in the range $0 \leq \phi \leq \pi$. Two related results, which are consequences of equations (26) and (27), are

$$\frac{D(|\zeta|^2)}{Dt} = -2\alpha|\zeta|^2 - 2\operatorname{Re}\{\zeta\zeta_p^*\} \tag{32}$$

and

$$\frac{D(\tan\phi)}{Dt} = -\alpha\tan^3\phi - \left(\alpha - \frac{\alpha_p}{\alpha}\right)\tan\phi - \frac{\tilde{\chi}_p}{\alpha}. \tag{33}$$

Because of the negative cubic term, there is always the tendency in the $\alpha > 0$ quarter-plane for the angle to decrease unless the pressure terms force it to behave to the contrary. Equations (26) and (27), however, are non-autonomous and, for Euler flows, there can be no question of α_p and $\tilde{\chi}_p$ remaining constant as the flow develops. Nevertheless certain tendencies can be discussed.

(1) In the left-hand quarter-plane equation where $\alpha < 0$ (7) shows that vorticity must be very small here. Initially if one starts in the region $\alpha < 0$ then equation (27) shows that χ can undergo rapid growth with $\phi \rightarrow \pi/2$. This is also reflected in equation (32) and equation (33) where the terms $-2\alpha|\zeta|^2$ and $-\alpha\tan^3\phi$ force rapid growth in $|\zeta|$ and $\tan\phi$ respectively. If χ increases in this way then (26) shows that there is also the tendency for α to increase also. Consequently there is a natural tendency for orbits to pass from the left- to the right-hand half-plane unless the pressure acts to prevent it.

(2) In the $\alpha > 0$ quarter-plane the opposite process occurs. Here, if $\alpha_p < \alpha^2$ and $\tilde{\chi}_p > 0$ for a sufficiently long time then $\phi \rightarrow 0$, which is the state of exact alignment. If $\alpha_p > \alpha^2$ then how far ϕ decreases depends upon specific values of α_p and $\tilde{\chi}_p$.

We conclude that the system has a natural tendency to reject negative values of α unless forced by the pressure Hessian to behave otherwise. This means that the system tends to prefer regions where stretching is positive. It is noteworthy that in rejecting the $\alpha < 0$ region an orbit must pass through the χ -axis into the region of $\alpha > 0$. This process can be reversed if the pressure behaves in a contrary manner but this behaviour can only be properly elucidated from data and this analysis is in progress.

What of exact solutions of the Euler equations? As we shall see in section 4, the Burgers vortex solution of the Euler equations is a Lagrangian fixed point of (26) and (27) with $\alpha = \text{constant}$, $\chi = 0$ with a corresponding angle $\phi = 0$. Hill’s spherical vortex, on the other hand, also has $\phi = 0$ but this does *not* correspond to a Lagrangian fixed point as fluid packets do not have values of α for which $D\alpha/Dt = 0$, based on the fact that $\mathbf{u} \cdot \nabla\alpha \neq 0$. To see this consider a vorticity field $\boldsymbol{\omega} = (\omega_r, \omega_\theta, \omega_z)$ where $\omega_r = \omega_z = 0$ and $\omega_\theta = Ar$ inside the sphere and zero outside it [52]. Then $\alpha = Az/5$, $\chi = 0$, $\alpha_p = A^2[4r^2 - \frac{10a^2}{3}]/50$ and $\chi_p = 0$. The solution for ABC flow for which $\mathbf{u} = \boldsymbol{\omega}$ with $u_1 = \omega_1 = \sin z + \cos y$, $u_2 = \omega_2 = \sin x + \cos z$, $u_3 = \omega_3 = \sin y + \cos x$, does not have constant values for α or χ . This means that neither ϕ is constant nor are the material derivatives of α and χ zero.

3. The stretching variables and the Navier–Stokes equations

For the Navier–Stokes equations, the task is to see how the addition of viscosity changes the two equations for α and χ in (24) and (25). In vorticity form the Navier–Stokes equations

are

$$\frac{D\omega_j}{Dt} = S_{jk}\omega_k + \nu\Delta\omega_j \quad (34)$$

and the equivalent of (7) for the scalar vorticity $\omega = |\boldsymbol{\omega}|$ is

$$\frac{D\omega}{Dt} = \alpha\omega + \nu\hat{\boldsymbol{\xi}} \cdot \Delta\boldsymbol{\omega}. \quad (35)$$

From the definition $\hat{\boldsymbol{\xi}} = \boldsymbol{\omega}/\omega$

$$\frac{D\xi_j}{Dt} = S_{jk}\xi_k - \alpha\xi_j + \frac{\nu}{\omega}\Delta\omega_j - \frac{\nu}{\omega}(\hat{\boldsymbol{\xi}} \cdot \Delta\boldsymbol{\omega})\xi_j. \quad (36)$$

It is convenient to turn derivatives of $\boldsymbol{\omega}$ into derivatives of $\hat{\boldsymbol{\xi}}$. To achieve this we use the fact that $\xi_j^2 = 1$ leading to $\xi_j\Delta\xi_j + |\nabla\xi_j|^2 = 0$. From the relations $\omega = \omega_j\xi_j$ and $\omega_j = \omega\xi_j$ we have

$$\Delta\omega = \omega|\nabla\hat{\boldsymbol{\xi}}|^2 + \hat{\boldsymbol{\xi}} \cdot \Delta\boldsymbol{\omega} \quad (37)$$

and

$$\frac{\Delta\omega_j}{\omega} = \Delta\xi_j + 2\nabla(\ln\omega) \cdot \nabla\xi_j + \xi_j\frac{\Delta\omega}{\omega}. \quad (38)$$

Dividing (37) by ω , multiplying by ξ_j and then adding to (38) enables us to rewrite (36) as

$$\frac{D\xi_j}{Dt} = S_{jk}\xi_k - \alpha\xi_j + \nu\Delta\xi_j + \nu|\nabla\hat{\boldsymbol{\xi}}|^2\xi_j + \nu\beta_j \quad (39)$$

where the vector $\boldsymbol{\beta}$ has components

$$\beta_j = \frac{\partial}{\partial x_k}(\ln|\boldsymbol{\omega}|^2)\frac{\partial\xi_j}{\partial x_k}. \quad (40)$$

$|\nabla\hat{\boldsymbol{\xi}}|$ is the ‘misalignment’ of the vector $\hat{\boldsymbol{\xi}}$ in the Frenet–Serret frame (see [50, 51] and the calculation in the appendix). Equation (40)[†] is the key to the calculations in the rest of this section because, apart from the logarithmic derivative in ω , it contains only $\hat{\boldsymbol{\xi}}$ and its derivatives. The strain matrix evolves according to

$$\frac{DS_{ij}}{Dt} = -S_{ik}S_{kj} - \frac{\omega_i\omega_j}{4} + \frac{|\boldsymbol{\omega}|^2\delta_{ij}}{4} - P_{ij} + \nu\Delta S_{ij} \quad (41)$$

and so,

$$\frac{D}{Dt}(S_{ij}\xi_j) = -P_{ij}\xi_j - \alpha S_{ij}\xi_j + \nu\{(\Delta S_{ij})\xi_j + S_{ij}\Delta\xi_j + |\nabla\hat{\boldsymbol{\xi}}|^2 S_{ij}\xi_j + S_{ij}\beta_j\}. \quad (42)$$

This, together with (39), can be combined to give,

$$\begin{aligned} \frac{D}{Dt}(\xi_i S_{ij}\xi_j) &= \chi^2 - \alpha^2 + 2\nu|\nabla\hat{\boldsymbol{\xi}}|^2\alpha + \nu\{\xi_i(\Delta S_{ij})\xi_j + \xi_i S_{ij}\Delta\xi_j + \Delta\xi_i S_{ij}\xi_j\} \\ &\quad + \nu\{\xi_i S_{ij}\beta_j + \beta_i S_{ij}\xi_j\} - \xi_i P_{ij}\xi_j. \end{aligned} \quad (43)$$

Out of the Laplacian terms in (43) it is desirable to form $\Delta\alpha$

$$\frac{D\alpha}{Dt} = \chi^2 - \alpha^2 + \nu\Delta\alpha + 2\nu|\nabla\hat{\boldsymbol{\xi}}|^2\alpha + \sum A_{jj} \quad (44)$$

where

$$A_{jl} = \nu(\xi_i S_{ij}\beta_l + \beta_i S_{ij}\xi_l) - 2\nu T_{jl} - \xi_j P_{ij}\xi_l \quad (45)$$

[†] This expression is not valid at stagnation points where $\omega = 0$; neither is $\hat{\boldsymbol{\xi}}$ defined at these.

and where T_{jl} is defined as

$$T_{jl} = \frac{\partial \xi_i}{\partial x_k} \frac{\partial S_{ij}}{\partial x_k} \xi_l + \frac{\partial \xi_i}{\partial x_k} S_{ij} \frac{\partial \xi_l}{\partial x_k} + \xi_i \frac{\partial S_{ij}}{\partial x_k} \frac{\partial \xi_l}{\partial x_k} \tag{46}$$

with β_i is defined in (40). We have isolated in (44) as many specific terms in α as possible and in forming the Laplacian term $\Delta\alpha$ we have separated the highest derivatives of S from the rest which lie in T_{jl} . For χ a similar result holds which is

$$\frac{D\chi_i}{Dt} = -2\alpha\chi_i + \nu\Delta\chi_i + 2\nu|\nabla\hat{\xi}|^2\chi_i + \varepsilon_{ijk}A_{kj}. \tag{47}$$

In summary, if we define

$$\mu_i = \varepsilon_{ijk}A_{kj} \quad \text{and} \quad \lambda = \sum A_{jj} \tag{48}$$

then equations (44) and (47) become

$$\frac{D\alpha}{Dt} = \chi^2 - \alpha^2 + \nu\Delta\alpha + 2\nu|\nabla\hat{\xi}|^2\alpha + \lambda \tag{49}$$

and

$$\frac{D\chi}{Dt} = -2\alpha\chi + \nu\Delta\chi + 2\nu|\nabla\hat{\xi}|^2\chi + \mu. \tag{50}$$

As in the Euler equations in section 2 this can be reduced to one equation in the scalar χ

$$\frac{D\chi}{Dt} = -2\chi\alpha + \nu\Delta\chi + \nu\left(2|\nabla\hat{\xi}|^2 - |\nabla\hat{\chi}|^2\right)\chi + \tilde{\mu} \tag{51}$$

where

$$\tilde{\mu} = \hat{\chi} \cdot \mu. \tag{52}$$

4. Burgers vortex and shear-layer solutions

We now postpone our discussion of the (α, χ) equations for the Navier–Stokes case until section 5 and return to the Burgers vortex and stretched shear-layer solutions. It is pertinent to ask whether equivalent Lagrangian fixed-point solutions exist for both the Euler and Navier–Stokes equations. Despite the caveats made in section 1, the simplicity of the Burgers solutions makes them candidates for this. In the following two subsections the basic formulae for the axisymmetric Burgers vortex (see [25, 13, 24, 35] and second note added in proof) and the Burgers shear layer (see [13, 24, 35]) are worked out. Then in section 4.3 we see how these are applied to the (α, χ) equations (49) and (50) for the Navier–Stokes equations and find that they do indeed correspond to fixed-point solutions. In the paper by Majda [13] a series of simple examples is given which includes pure rotation, a swirling drain and the two Burgers solutions (see [13, section 1C]). The two expressions for the vorticity $\omega(\mathbf{x}, t)$ for the latter pair of examples are based on an N -dimensional heat kernel but for the sake of simplicity in the following two subsections we use the time asymptotic limit of this.

4.1. Burgers vortices

Consider a strain field $\mathbf{u} = (-\frac{\gamma x}{2}, -\frac{\gamma y}{2}, \gamma z)^T$ with a superimposed two-dimensional velocity field $(-yf(r), xf(r), 0)^T$ where the function $f(r)$ will be fixed later on. The variable r is given by $r^2 = x^2 + y^2$. Then the full velocity field is

$$\mathbf{u} = \left(-\frac{\gamma x}{2} - yf(r), -\frac{\gamma y}{2} + xf(r), \gamma z\right)^T \tag{53}$$

and it is easily seen that the vorticity is

$$\boldsymbol{\omega} = (0, 0, \omega_3)^T \quad (54)$$

where $\omega_3 = 2f + rf'$. Moreover the strain-matrix S is given by

$$S = \begin{pmatrix} -\frac{\gamma}{2} - \frac{xyf'}{r} & \frac{(x^2-y^2)f'}{2r} & 0 \\ \frac{(x^2-y^2)f'}{2r} & -\frac{\gamma}{2} + \frac{xyf'}{r} & 0 \\ 0 & 0 & \gamma \end{pmatrix} \quad (55)$$

Immediately we see that $\mathbf{e}_3 = (0, 0, 1)^T$ and $\lambda_3 = \gamma$ and the other two eigenvalues can easily be computed

$$\lambda_{1,2} = \frac{-\gamma \pm rf'}{2} \quad (56)$$

with their corresponding eigenvectors lying in the horizontal plane. Now for the Euler equations one can simply take $f = \frac{1}{r^2} \int_0^r s \omega_3(s) ds$ and so $\boldsymbol{\omega} = (0, 0, \omega_3(r))^T$. For instance, there is a solution of the three-dimensional Euler equations on compact support whose amplitude increases exponentially while its support decreases exponentially [19].

For the Navier–Stokes equations, however, there exists a form of $f(r)$ in which dissipation and stretching balance which, in the limit $t \rightarrow \infty$, is given by [13]

$$f(r) = \frac{1 - \exp(-ar^2)}{r^2} u_0. \quad (57)$$

where $a = \gamma/4\nu$. This is a profile which has its maximum when $r = 0$. Note that when $r = 0$ then $f(0) = a$, $\omega_3(0) = 2a$ whereas $[rf'(r)]_{r=0} = 0$. Near $r = 0$, $rf' \sim -2a^2r^2 < 0$ and so we have two negative eigenvalues and one positive for this form of solution. Also the total strain at $r = 0$ is

$$\sum_{i,j} S_{ij}^2 = \frac{1}{2}(3\gamma^2 + (rf')^2)_{r=0} = \frac{3\gamma^2}{2}. \quad (58)$$

Hence if $\nu \ll 1$ then $a \gg \gamma$ and so the vorticity $\omega_3(0) = 2a$ is much larger than the total strain. An $x - y$ plane contrast cross-section of the vorticity field for a Burgers vortex is produced in figure 1(a).

4.2. The Burgers shear-layer solution

Consider a jet $\mathbf{u} = (0, -\gamma y, \gamma z)^T$ which compresses in the y -direction but expands in the z -direction. Now impose a velocity field $v(y)$ on the x -direction so that

$$\mathbf{u} = (v(y), -\gamma y, \gamma z)^T \quad (59)$$

$$\boldsymbol{\omega} = (0, 0, \omega_3)^T \quad (60)$$

where $\omega_3 = -v'(y)$. For the Navier–Stokes equations, in the limit $t \rightarrow \infty$, if $v(y)$ is taken to be

$$v(y) = \frac{1}{\sqrt{2\pi}} \int_{-\infty}^{y\sqrt{2a}} v(0) \exp(-s^2) ds \quad (61)$$

with $a = \gamma/4\nu$ then

$$\omega_3 = \sqrt{\frac{2a}{\pi}} \exp(-2ay^2) \int \omega_0(s) ds. \quad (62)$$

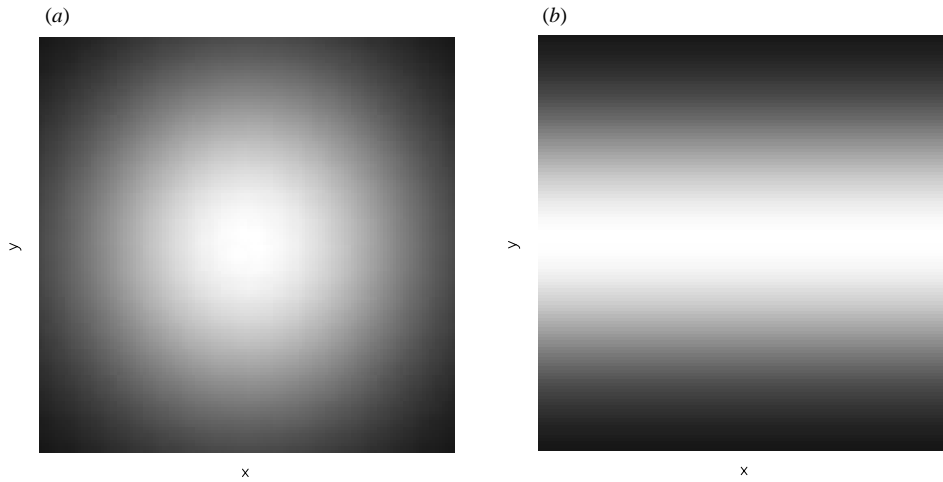


Figure 1. (a) The $x - y$ cross section of a Burgers vortex with the z -coordinate pointing out of the paper in which direction the vorticity vector, $\omega = (0, 0, \omega_3)^T$, points. The whiter the area the higher the vorticity. (b) The $x - y$ cross section of a Burgers stretched shear layer. As in (a), the z -coordinate points out of the paper in which direction the vorticity vector, $\omega = (0, 0, \omega_3)^T$, points. The whiter the area the higher the vorticity.

This the *Burgers shear-layer* for which the strain matrix S is given by

$$S = \begin{pmatrix} 0 & \frac{v'}{2} & 0 \\ \frac{v'}{2} & -\gamma & 0 \\ 0 & 0 & \gamma \end{pmatrix}. \tag{63}$$

As before we see that $e_3 = (0, 0, 1)^T$ and $\lambda_3 = \gamma$ and the other two eigenvalues are

$$\lambda_{1,2} = \frac{-\gamma \pm (\gamma^2 + v'^2)^{1/2}}{2} \tag{64}$$

with their corresponding eigenvectors lying in the horizontal plane. In this case the total strain is

$$\sum_{i,j} S_{ij}^2 = 2\gamma^2 + \frac{v'^2}{2}. \tag{65}$$

When $v \ll 1$ then $a \gg \gamma$ and therefore $|v'|^2 \gg \gamma^2$. Hence when the vorticity is high then so is the total strain, in contrast with the vortex tube in the previous subsection. An $x - y$ plane contrast cross section of the vorticity field for a Burgers stretched shear layer is produced in figure 1(b),

4.3. The (α, χ) equations for both tube and shear layer

Taking the third component of the velocity version of the Navier–Stokes equations it is easy to show in both the above cases

$$\frac{\partial p}{\partial z} = -\gamma z \tag{66}$$

and hence

$$\alpha_p = -\gamma^2 \quad \chi_p = 0. \tag{67}$$

In addition, using the solution for ω and the form of S , in both cases

$$\alpha = \gamma \quad \chi = 0 \quad (68)$$

with corresponding angle

$$\phi = 0 \quad (69)$$

reflecting the fact that there is exact alignment between ω and e_3 with this fixed point sitting on the α -axis. Clearly, in terms of the angle *we can make no distinction between the tube and the shear layer*, nor is there any distinction between the cases of alignment or anti-alignment of ω and an eigenvector of S . Moreover, the unit vectors $\hat{\xi}$ and $\hat{\chi}$ are given by $\hat{\xi} = \hat{k}$ and $\hat{\chi} = 0$ so $\nabla \hat{\xi} = 0$. This means that when $\mu = 0$ and $\lambda = \gamma^2$, the relevant (α, χ) equations given in (49) and (50) are satisfied by equations (67) and (68) for which

$$\frac{D\alpha}{Dt} = 0 \quad \frac{D\chi}{Dt} = 0. \quad (70)$$

The problem of stability is considered in the next section; there we will show that this fixed point is indeed stable provided λ and μ remain constant. Given the fact that both Burgers cases are essentially two-dimensional velocity fields superimposed on three-dimensional strain fields, any example of this type will produce a strain matrix S with a similar block diagonal form as in (55) and (63) with a corresponding eigenvector e_3 which is parallel to the vorticity vector ω . All examples of this type therefore have $\phi = 0$. Moffatt *et al* [25] have used asymptotics on the Burgers vortex where they allow a certain small asymmetry from the axisymmetric solution (57) but they point out that only the exact symmetric solution is known.

What is not proved, however, is that if the system is attracted to a stable Lagrangian fixed-point solution with an orientation near $\phi = 0$ then this must automatically correspond to either of the Burgers-like solutions sketched above; there may be other unknown structures which fall into this category (see the comments at the end of section 2 on Hill's spherical vortex). The lack of certainty in the topology reflects the problem of not having enough dynamic angles in the system.

5. A mechanism for the formation of thin structures in Navier–Stokes flows

So far we have made no assumptions. Let us now discuss some approximations and put forward the following theoretical picture which is consistent with the formation of thin structures in isotropic Navier–Stokes turbulence. Over all calculations of this type lies the heavy shadow of the technical question of regularity, which is still an open problem. The fact that alignment in mature turbulent flows is being discussed, however, means that a sufficient degree of regularity is being imputed to the solutions anyway. From now on we assume that the flow is regular and that all the necessary quantities are bounded. From section 4 we know that when the flow assumes a Burgers structure, λ and μ take the values

$$\lambda = \gamma^2 \quad \mu = 0. \quad (71)$$

In the following, however, we do *not* assume that λ and μ take the values given in (71) as this is tantamount to assuming the answer. Nevertheless, the highly simplified form that λ and μ take when the flow assumes a Burgers state motivates us to *assume that the variables α , μ , λ and μ have reached a simultaneous equilibrium in some connected region of vorticity whose growth has been controlled by dissipation*. First, we want to see if the ‘fixed point’ values taken by α and χ at this equilibrium correspond to a small angle ϕ_0 and

secondly whether this fixed point is stable. To investigate this stability question we begin by assuming that λ and μ are constant in the four equations in (49) and (50)

$$\frac{D\alpha}{Dt} = \chi^2 - \alpha^2 + \nu\Delta\alpha + \lambda \tag{72}$$

$$\frac{D\chi}{Dt} = -2\alpha\chi + \nu\Delta\chi + \mu \tag{73}$$

where, for reasons of simplicity, we have written these without the quantity $|\nabla\hat{\xi}|^2$. These terms are the least important and are dealt with later in the appendix. Fixed points in (α_0, χ_0) occur at

$$2\alpha_0^2 = \lambda + \sqrt{\mu^2 + \lambda^2} \quad \chi_{i,0} = \frac{\mu_i}{2\alpha_0} \tag{74}$$

where $\mu = |\mu|$. Hence there are two fixed points in four-space, corresponding to the two roots of α_0 in (74). Without the Laplacian term it is easy to show that the eigenvalue stability problem is

$$(\Lambda + 2\alpha_0)^2[(\Lambda + 2\alpha_0)^2 + 4\chi_0^2] = 0 \tag{75}$$

thereby giving the four roots

$$\Lambda = -2\alpha_0 \text{ (twice)} \quad \Lambda = -2(\alpha_0 \pm i\chi_0). \tag{76}$$

These roots correspond to an unstable fixed point for the negative root for α_0 and a stable one for the positive root. In the latter case, there is exponential contraction in two of the directions in the four-space with a stable spiral in the other two directions. When the Laplacian is included we look at the stability of linearized solutions of the type $\exp(i\mathbf{k} \cdot \mathbf{x} + \Lambda t)$ around (α_0, χ_0) . The only difference this makes to (76) is that $2\alpha_0 \rightarrow 2\alpha_0 + \nu k^2$. We conclude that provided $\alpha_0 > 0$ the equilibrium solution is stable to the disturbance of all wavenumbers. For the half-plane the two fixed points are

$$\sqrt{2}\alpha_0 = \pm \left[\lambda + \sqrt{\mu^2 + \lambda^2} \right]^{1/2} \quad \sqrt{2}\chi_0 = \left[-\lambda + \sqrt{\mu^2 + \lambda^2} \right]^{1/2}. \tag{77}$$

The stable spiral is shown in figure 2 which is projected onto the variables χ_1 and α . Defining m to be

$$m = \frac{\mu}{|\lambda|} \tag{78}$$

the angle ϕ_0 corresponding to the stable fixed point is (the + sign is for $\lambda > 0$ and the – sign for $\lambda < 0$)

$$\tan \phi_0^\pm = \frac{\sqrt{m^2 + 1} \mp 1}{m} \tag{79}$$

which can be simplified to

$$\tan 2\phi_0^\pm = \pm m. \tag{80}$$

Now the exact Burgers solutions both correspond to $m = 0$ and, because $\alpha = \gamma > 0$, they correspond to an *attracting* fixed point of the system. We note, however, that when it takes nonzero values, m is dependent only on the *ratio* of μ and $|\lambda|$. Although we have no hard information on the magnitude of m , in fact the angle ϕ_0^+ is relatively insensitive to this magnitude. For $\lambda > 0$, if $m \approx 0$ then $\phi_0^+ \approx 0$ but if $m \approx 1$ then $\phi_0^+ \approx \pi/8$. Even if $m = \infty$ then $\phi_0^+ = \pi/4$. Hence at worst, ϕ_0^+ lies in a 45° cone. Therefore, even when $m > 0$ we are still close to alignment. More generally, μ and λ derive respectively from forming the vector and scalar products of the same set of functions so, in an isolated region

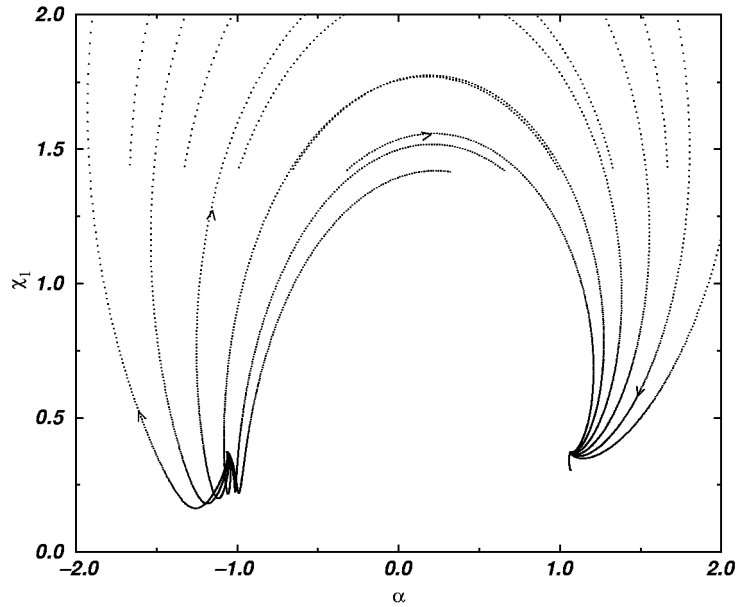


Figure 2. Orbits in the α - χ phase space projected onto the α - χ_1 plane. The spiral structure at the two fixed points is just evident.

of vorticity Ω , we might expect that on the spatial average over a random set of points in Ω , m would take the value $m \approx 1$. It is also possible that because μ is formed from a cross product while λ is formed from a dot product then at the natural angle of alignment the μ term would be the weaker of the two making $m < 1$. We therefore conclude that, over the spatial average within a small intense region for $\lambda > 0$,

$$\phi_0^+ \approx \pi/8 \quad (81)$$

but that ϕ_0^+ may indeed be somewhat smaller than this. Experiments [29–32] and simulations [14, 16, 18, 26, 20, 28] generally measure the cosine of the angle ϕ , often observing that a bunching around $\cos \phi \approx 1$ in their PDFs is a demonstration of alignment. For $\phi_0^+ \approx \pi/8$ we have

$$\cos \phi_0^+ \approx 0.92. \quad (82)$$

This value of m therefore produces fairly close alignment. This is consistent with the region finding an equilibrium shape near to a thin Burgers-like structure (for which the exact value of m is zero) which corresponds to $\lambda > 0$. When $\lambda < 0$, however,

$$\phi_0^- = \pi/2 - \phi_0^+ \quad (83)$$

and the equivalent value of ϕ_0^- is $3\pi/8$. Hence vortex lines are badly misaligned in this case.

6. Conclusion

The thin vortical structures which are observed in numerical simulations of turbulence have been one of the most intriguing visual manifestations of the complexity for which turbulence, for better or for worse, has become a byword in the last two decades. Our

results are consistent with near Burgers-like structures (see figure 1) forming out of those connected parts of the flow where λ and μ equilibrate and where $\lambda > 0$. The fact that the stable equilibrium occurs in a region of $\alpha_0 > 0$ means that there is a preference for vortex stretching [1, 14, 53]. To say that these regions consist of precisely tubes and/or sheets is to oversimplify the matter; more generally the individual structures probably have a fractal dimension which lies somewhere between one and two corresponding to tubes and between two and three corresponding to sheets [2–4, 54]. Nevertheless, tubes and sheets as extreme limits of the topology suffice as an approximate description despite the fact that their local interactions and constant metamorphosis produces levels of geometric complexity which are beyond our understanding at the moment. This raises several questions regarding the geometric consequences of vorticity alignment.

(1) Can all solutions for which $\phi \approx 0$, which are also Lagrangian fixed points of the (α, χ) equations, be categorized as ‘thin’ in the sense that they are quasi one-dimensional or two-dimensional? While we have characterized these structures by the angle $\phi_0(x, t)$ which lies between ω and $S\omega$, are there other dynamic angles which characterize the topology more specifically?

(2) Are the Burgers solutions or their generalizations unique among the set of thin solutions?

(3) What is the behaviour of $m = \mu/|\lambda|$ defined in (78) and what determines the sign of λ ? The assumption that λ and μ are roughly constant in some regions is based on the assumption that (consistent with the fact that they behave this way for the two Burgers solutions) a balance occurs at the deepest scales between the pressure and the viscous terms expressed through $P, S, \nabla S$ and $\nabla\omega$. Such an assumption would be hard to prove directly while no regularity proof exists.

(4) How are α and χ affected when there are local interactions; for instance, when two sheets interact and wrap up to become tubes [26]? It is possible that large values of λ correspond more to sheets than tubes since the former have higher strain. The experiments of Andreotti *et al* [36] creating Burgers vortices suggest that the tubes formed from the roll-up of sheets have a long lifetime compared with the roll-up time. This suggests that two time scales may be involved; the first being the time it takes for the orbit in (α, χ) space to stabilize and the second the time over which λ and μ remain constant before themselves decaying due to dissipative effects.

(5) What role does the Hessian matrix P play in these processes? Is there a consistent pattern in the sign of α_p ?

As far as (1) is concerned, it is clear that one angle is by no means sufficient to adequately describe the topology. There are two other apparent natural angles in the system. The first of these is based on the matrix $\omega_{i,j}$ instead of S_{ij} which we discuss only in the Euler case. Define

$$\alpha^{(\omega)} = \frac{\omega_i \omega_{i,j} \omega_j}{\omega \cdot \omega} = \frac{\omega \cdot (\omega \cdot \nabla)\omega}{\omega \cdot \omega} \tag{84}$$

and then use the general result (12) to show that

$$\frac{D\alpha^{(\omega)}}{Dt} = \omega \cdot \nabla\alpha. \tag{85}$$

Equation (85) shows that points moving with the flow in regions where $\alpha = \text{constant}$ (or even just spatially independent) also have $\alpha^{(\omega)}$ as a constant of the motion. Now define

$$\chi^{(\omega)} = \frac{\omega \times (\omega \cdot \nabla)\omega}{\omega \cdot \omega} \tag{86}$$

then

$$\frac{D\chi^{(\omega)}}{Dt} = (\omega \cdot \nabla)\chi + 2\alpha^{(\omega)}\chi - 2\alpha\chi^{(\omega)} + \frac{2\sigma \times (\omega \cdot \nabla)\omega}{\omega \cdot \omega}. \quad (87)$$

When $\phi = 0$ then $\sigma = S\omega = \alpha\omega$ and $\chi = 0$ and so

$$\frac{D\chi^{(\omega)}}{Dt} = 0. \quad (88)$$

In consequence the angle ψ between ω and $(\omega \cdot \nabla)\omega$ for points travelling with the flow is given by

$$\tan \psi = \frac{\text{constant}}{\alpha^{(\omega)}}. \quad (89)$$

ψ therefore decreases in regions where $\alpha^{(\omega)}$ is stretching. The second angle concerns the Hessian matrix of the pressure P

$$\tan \phi_P = \frac{|\omega \times P\omega|}{\omega \cdot P\omega} \quad (90)$$

but we have no separate knowledge of the evolution of P . In fact P and S are less independent than one would think. A consequence of equation (23) is that when ω aligns with an eigenvector of S then ω also aligns simultaneously with an eigenvector of P .

The lack of knowledge of m raised in (3) above is balanced in part by the insensitivity of ϕ_0 , the attracting angle, to the value of m through the relation ($\lambda > 0$)

$$\tan 2\phi_0^+ = m. \quad (91)$$

There is no reason, *a priori*, why exact alignment at $m = 0$ should be attracting. Nevertheless, values of $m > 0$ produce attracting orientations which are still close enough to alignment to suggest that we are near a thin structure which we conjecture is perhaps twisted in some way. As we showed in the last section, different regions may take different spatial values of m but their associated angles may still be close enough to look the same in observations or simulations. Geometrical information about the local and relative orientation of vortex lines in the sense of the Frenet–Serret equations [50, 51] is obviously contained in m , but these need information on $\nabla\omega$ which we do not have. It is possible that more can be said about m using a scaling argument.

What the formulation of this paper does not do is differentiate between tubes and sheets; the alignment process is the same for both and we have no other information which distinguishes them. In fact, one very important set of processes, not accounted for by the dynamics of ϕ alone, are the interaction processes between one sheet and another. The Kelvin–Helmholtz instability, which is an Euler phenomenon, is a well known mechanism through which it is thought that two dimensional sheet-like objects wrap up to become tubes [38, 26, 27, 20, 55]. Such local interaction processes are extremely subtle and if they are to be accounted for dynamically then certainly more than one angle would be needed.

The thin structures observed in simulations take up no more than a few per cent of the total flow volume indicating that vorticity is not distributed evenly. This may be one of the reasons behind the failure to prove regularity. The methods used have been based upon attempts to control the *global* enstrophy, $\int_{\Omega} |\omega|^2 dV$, which have foundered on the problem of the dissipation being too weak to control the estimated nonlinear terms (see references in [56]). These latter terms have their origin in the vortex stretching term, $\int \omega_j S_{ij} \omega_j dV$, and have to be estimated by standard Sobolev inequalities. The failure to control the global enstrophy for more than a finite time by this method probably has its origins in the use of volume integration in which L^2 -norms average over, and perhaps miss, the spatial structures

where the nonlinearity has been strongly depleted by alignment. Constantin’s Biot–Savart integral formula for α in terms of a triad of vectors related to $\hat{\xi}$ illustrates how nonlinearity is depleted inside the volume integral when significant alignment takes place [40].

The general picture that emerges from this analysis is that the variables (α, χ) seem to form a natural pair of variables in which to express the dynamics of vortex formations. In both the Euler and Navier–Stokes cases negative values of α are repelling and, without interference from the pressure, ϕ would limit to zero. Any initial state corresponding to a negative value of α would require the system to go through the $\phi = \pi/2$ stage before becoming a Burgers-like shear layer or tube if indeed it is driven that far. The difference between the two is that for the Euler equations there is no stable equilibrium point provided by the viscosity and the whole process could reverse, although Ohkitani and Kishiba [47] report that they observe an alignment between ω and the third eigenvector of P . A systematic study of simulation data for the three-dimensional Euler equations is underway to understand the properties of the more general behaviour of the Hessian matrix P .

One curious conclusion from (26) in the Euler equation case, for a Lagrangian particle element initially at $\mathbf{X} = \mathbf{x}(0)$, is that if $\alpha(\mathbf{X}, 0) < 0$ and $\phi(\mathbf{X}, t) < \pi/4$ with $\alpha_p > 0$ then $\alpha \rightarrow -\infty$ in a finite time. In contrast, if $\alpha(\mathbf{X}, 0) > 0$ and $\phi(\mathbf{X}, t) > \pi/4$ with $\alpha_p < 0$ then $\alpha \rightarrow \infty$ in a finite time. This is consistent with the results of Ng and Battercharjee [57] who have studied the Euler equations under high-symmetry conditions which makes the problem quasi one dimensional.

Past simulations have shown that initially ω aligns with the largest eigenvector of S but as the turbulence becomes more mature ω aligns with the second eigenvector [14, 16, 26] as a global average. Tsinober *et al* [32] have recently reported, however, that *locally* they see significant alignments between ω and *both* the first and the second eigenvectors of S . They also report that the vorticity does not have to be too intense and they produce evidence to suggest that the background field is not Gaussian.

Acknowledgments

We are grateful to Charles Doering, Robert Kerr, Andrew Majda, Itamar Procaccia, Len Sander, Edriss Titi and Arkady Tsinober for several helpful suggestions. JDG gratefully thanks the trustees of the Sir Siegmund Warburg Foundation in London for their financial support during his nine-month stay at the Weizmann Institute of Science. MH is thankful to the UK EPSRC Mathematics Committee for the award of a studentship.

Appendix. The effect of the misalignment terms

For the $|\nabla\hat{\xi}|^2$ terms left out of the discussion in section 5, it would be preferable if we had five evolution equations in α , χ_i and $\nabla\hat{\xi}$ and not just four but we have been unable to discover any delicate cancellations in the material derivative of the last variable. Instead, we include this as a constant term in the equilibrium-point analysis above. For a vortex line, $\nabla\hat{\xi}$ is called the misalignment and plays an interesting role. Constantin *et al* [50] note that

$$|\nabla\hat{\xi}|^2 = |(\hat{\xi} \cdot \nabla)\hat{\xi}|^2 + |(\hat{n} \cdot \nabla)\hat{\xi}|^2 + |(\hat{b} \cdot \nabla)\hat{\xi}|^2 \tag{92}$$

where the first term on the right-hand side of (92) is the square of the curvature and the second and third are the squares of the lack of parallelity between a vortex line and

neighbouring lines in the normal (\hat{n}) and binormal (\hat{b}) directions respectively. Galanti et al [51] have produced theoretical and numerical arguments which indicate that the stronger the vorticity and the greater the curvature of a vortex line the stronger the stretching and therefore the more liable it is to straighten. To show how this is the case we define

$$a = \nu |\nabla \hat{\xi}|^2 \quad \tilde{\alpha} = \alpha - a \quad \tilde{\lambda} = \lambda + a^2. \quad (93)$$

The (α, χ) equations become

$$\frac{D\tilde{\alpha}}{Dt} = \chi^2 - \tilde{\alpha}^2 + \tilde{\lambda} \quad (94)$$

$$\frac{D\chi}{Dt} = -2\tilde{\alpha}\chi + \mu. \quad (95)$$

The stability problem is unchanged and fixed points come from

$$\tilde{\alpha}_0^2 = \frac{\tilde{\lambda} + (\tilde{\lambda}^2 + \mu^2)^{1/2}}{2}. \quad (96)$$

From (96), $\tilde{\alpha}_0^2 \geq \tilde{\lambda} \geq a^2$ when $\lambda > 0$ and so $\alpha_0 \geq 2a$ for positive values of α_0 . Moreover, when considering the angle of orientation of the equilibrium point $\tilde{\phi}_0$ we see that

$$\tan 2\tilde{\phi}_0 = \frac{|\mu|}{|\tilde{\lambda}|} = \frac{|\mu|}{|\lambda + a^2|} \leq m. \quad (97)$$

Hence

$$\tan 2\tilde{\phi}_0 \leq \tan 2\phi_0. \quad (98)$$

Equation (98) shows that nonzero values of $|\nabla \hat{\xi}|^2$ act to make the angle smaller than when it is excluded. Of course the angle ϕ and $|\nabla \hat{\xi}|^2$ are different ways of expressing the same effect. We actually need another differential equation to form an accurate picture and this, in turn, needs information on ∇S and $\nabla \omega$. The above calculation shows that for the (α, χ) equations alone large values of $|\nabla \hat{\xi}|^2$ force stronger alignment in ϕ , thereby confirming the effect seen in [51].

Note added in proof 1. In a private communication, P Constantin has informed us that the result in equation (10) has been known privately in unpublished form since 1983.

Note added in proof 2. See also the paper by Andreotti B (1997) Studying Burgers' models to investigate the physical meaning of the alignments statistically observed in turbulence *Phys. Fluids A* **9** 735–42.

References

- [1] Taylor G I 1938 Production and dissipation of vorticity in a turbulent fluid *Proc. R. Soc. A* **164** 15–23
- [2] Chorin A 1982 The evolution of a turbulent vortex *Commun. Math. Phys.* **83** 517
- [3] Frisch U 1995 *Turbulence: The Legacy of A N Kolmogorov* (Cambridge: Cambridge University Press)
- [4] Frisch U, Sulem P-L and Nelkin M 1978 A simple dynamical model of intermittent fully developed turbulence *J. Fluid Mech.* **87** 719–36
- [5] Townsend A A 1951 On the fine scale structure of turbulence *Proc. R. Soc. A* **208** 534–42
- [6] Batchelor G K 1953 *Homogeneous Turbulence* (Cambridge: Cambridge University Press)
- [7] Siggia E D 1981 Numerical study of small scale intermittency in three-dimensional turbulence *J. Fluid Mech.* **107** 375–406
- [8] Moffatt H K 1981 Some developments in the theory of turbulence *J. Fluid Mech.* **106** 27

- [9] Moffatt H K 1993 Spiral structures in turbulent flow *Fractals, Wavelets and Fourier transforms: New Developments and New Applications* ed M Farge, J C R Hunt and J C Vassilicos (Oxford: Clarendon) pp 317–24
- [10] Lundgren T 1982 Strained spiral vortex model for turbulent fine structure *Phys. Fluids* **25** 2193–203
- [11] Lin S J and Corcos G 1984 The mixing layer: deterministic models of turbulent flow. Part 3. The effect of plane strain on the dynamics of streamwise vortices *J. Fluid Mech.* **141** 139–78
- [12] Neu J C 1984 The dynamics of stretched vortices *J. Fluid Mech.* **143** 253–76
- [13] Majda A 1986 Vorticity and the mathematical theory of incompressible fluid flow *Commun. Pure Appl. Math.* **39** 187
- [14] Ashurst W, Kerstein W, Kerr R and Gibson C 1987 Alignment of vorticity and scalar gradient with strain rate in simulated Navier–Stokes turbulence *Phys. Fluids* **30** 2343
- [15] Ashurst W, Chen J Y and Rogers M M 1987 Pressure gradient alignment with strain rate and scalar gradient in simulated Navier–Stokes turbulence *Phys. Fluids* **30** 3293
- [16] She Z-S, Jackson E and Orszag S 1990 Intermittent vortex structures in homogeneous isotropic turbulence *Nature* **344** 226–8
- [17] Hosokawa I and Yamamoto K 1990 Intermittency of dissipation in fully developed isotropic turbulence *J. Phys. Soc. Japan* **59** 401–4
- [18] Vincent A and Meneguzzi M 1991 The spatial and statistical properties of homogeneous turbulence *J. Fluid Mech.* **225** 1–20
- [19] Majda A 1991 Vorticity, turbulence and acoustics in fluid flow *SIAM Rev.* **33** 349
- [20] Ruetsch G R and Maxey M R 1991 Small scale features of vorticity and passive scalar fields in homogeneous isotropic turbulence *Phys. Fluids A* **3** 1587–97
- [21] Douady S, Couder Y and Brachet M E 1991 Direct observation of the intermittency of intense vortex filaments in turbulence *Phys. Rev. Lett.* **67** 983
- [22] Tanaka M and Kida S 1993 Characterization of vortex tubes and sheets *Phys. Fluids A* **5** 2079–82
- [23] Kida S 1993 Tube-like structures in turbulence *Lect. Notes Numer. Appl. Anal.* **12** 137–59
- [24] Saffman P G 1993 *Vortex Dynamics* (Cambridge: Cambridge University Press)
- [25] Moffatt H K, Kida S and Ohkitani K 1994 Stretched vortices—the sinews of turbulence; large-Reynolds-number asymptotics *J. Fluid Mech.* **259** 241
- [26] Vincent A and Meneguzzi M 1994 The dynamics of vorticity tubes of homogeneous turbulence *J. Fluid Mech.* **225** 245–54
- [27] Passot T, Politano H, Sulem P L, Angilella J R and Meneguzzi M 1995 Instability of strained vortex layers and vortex tube formation in homogeneous turbulence *J. Fluid Mech.* **282** 313
- [28] Blackburn H M, Mansour N N and Cantwell B J 1996 Topology of fine-scale motions in turbulent channel flow *J. Fluid Mech.* **310** 269–92
- [29] Tsinober A, Kit E and Dracos T 1992 Experimental investigation of the field of velocity gradients in turbulent flows *J. Fluid Mech.* **242** 169
- [30] Tsinober A, Eggels J and Nieuwstadt F 1995 On alignments and small scale structure in turbulent pipe flow *Fluid Dynam. Res.* **16** 297
- [31] Tsinober A 1996 Geometrical Statistics in Turbulence *6th Eur. Turbulence Conf. (EuroMech) (Lausanne, Switzerland July 2–5th)*
- [32] Tsinober A, Shtilman L and Vaisburd H 1997 A study of properties of vortex stretching and enstrophy generation in numerical and laboratory turbulence *Fluid Dynam. Res.* **20** to appear
- [33] Jiminez J 1992 Kinematic alignments in turbulent flows *Phys. Fluids A* **4** 652–4
- [34] Dresselhaus E and Tabor M 1991 The kinematics of stretching and alignment of material elements in general flow fields *J. Fluid Mech.* **236** 415
- [35] Burgers J M 1948 A mathematical model illustrating the theory of turbulence *Adv. Appl. Math.* **1** 1
- [36] Andreotti B, Douady S and Couder Y 1997 About the interaction between vorticity and stretching in coherent structures *Turbulence Modeling and Vortex Dynamics (Lecture Notes in Physics 491)* ed O Boratav *et al* (Heidelberg: Springer) pp 92–108
- [37] Kerr R 1993 Evidence for a singularity of the 3-dimensional, incompressible Euler equations *Phys. Fluids A* **5** 1725
- [38] Kerr R 1993 The role of singularities in turbulence in *Unstable Turbulent Fluid Motion* ed S Kida (Singapore: World Scientific) p 102
- [39] Constantin P, Fefferman Ch and Majda A 1996 Geometric constraints on potentially singular solutions for the 3-D Euler equations *Commun. Partial Diff. Equations* **21** 559
- [40] Constantin P 1994 Geometric statistics in turbulence *SIAM Rev.* **36** 73
- [41] Boratav O N and Pelz R B 1994 Direct numerical simulation of transition to turbulence from a high-symmetry

- initial condition *Phys. Fluids A* **6** 2757–84
- [42] Cantwell B J 1992 Exact solution of a restricted Euler equation for the velocity gradient tensor *Phys. Fluids A* **4** 782
- [43] Beale J T, Kato T and Majda A 1984 Remarks on the breakdown of smooth solutions for the 3-D Euler equations *Commun. Math. Phys.* **94** 61
- [44] Gibbon J D and Heritage M 1997 Angular dependence and growth of vorticity in the 3D Euler equations *Phys. Fluids A* **9** 901–9
- [45] Constantin P and Fefferman Ch 1993 Direction of vorticity and the problem of global regularity for the Navier–Stokes equations *Indiana Univ. J.* **42** 775
- [46] Ohkitani K 1993 Eigenvalue problems in three-dimensional Euler flows *Phys. Fluids A* **5** 2570
- [47] Ohkitani K and Kishiba S 1995 Nonlocal nature of vortex stretching in an inviscid fluid *Phys. Fluids A* **7** 411
- [48] Vieillefosse P 1984 Internal motion of a small element of fluid in an inviscid flow *Physica A* **125** 837
- [49] Cheng W-P and Cantwell B J 1996 Study of the velocity gradient tensor in turbulent flow, Stanford University: Ames research Center, Joint Institute for Aeronautics and Acoustics, TR 114
- [50] Constantin P, Procaccia I and Segel D 1995 Creation and dynamics of vortex tubes in three-dimensional turbulence *Phys. Rev. E* **51** 3207
- [51] Galanti B, Procaccia I and Segel D 1996 Dynamics of vortex lines in turbulent flows *Phys. Rev. E* **54** 5122
- [52] Batchelor G K 1975 *Fluid Dynamics* (Cambridge: Cambridge University Press)
- [53] Lund T S and Rogers M M 1994 *Phys. Fluids* **6** 1838–47
- [54] Gibbon J D 1995 A conjecture regarding local behaviour of vorticity in the 3D incompressible Navier–Stokes equations *Phys. Lett. A* **203** 181–8
- [55] Kishiba S, Ohkitani K and Kida S 1994 Interaction of helical modes in the formation of vortical structures in decaying isotropic turbulence *J. Phys. Soc. Japan* **63** 2135
- [56] Doering C R and Gibbon J D 1995 *Applied Analysis of the Navier–Stokes Equations* (Cambridge: Cambridge University Press)
- [57] Ng C S and Bhattacharjee A 1996 Sufficient condition for a finite time singularity in a high symmetry Euler flow: analysis and statistics *Phys. Rev. E* **54** 1530–4